# Near-unity indistinguishability single photon source for large-scale integrated quantum optics

Łukasz Dusanowski,[1,*] Soon-Hong Kwon,[1,2] Christian Schneider,[1] and Sven Höfling[1,3]

[1] *Technische Physik, University of Würzburg, Physikalisches Institut and Wilhelm-Conrad-Röntgen-Research Center for Complex Material Systems, Am Hubland, D-97074 Würzburg, Germany*

[2] *Department of Physics, Chung-Ang University, 156-756 Seoul, Korea*

[3] *SUPA, School of Physics and Astronomy, University of St Andrews, KY16 9SS St Andrews, UK*

(Dated: February 25, 2019)

Integrated single photon sources are key building blocks for realizing scalable devices for quantum information processing. For such applications highly coherent and indistinguishable single photons on a chip are required. Here we report on a triggered resonance fluorescence single photon source based on In(Ga)As/GaAs quantum dots coupled to single- and multi-mode ridge waveguides. We demonstrate the generation of highly linearly polarized resonance fluorescence photons with 99.1% (96.0%) single-photon purity and 97.5% (95.0%) indistinguishability in case of multi-mode (single-mode) waveguide devices fulfilling the strict requirements imposed by multi-interferometric quantum optics applications. Our integrated triggered single photon source can be readily scaled up, promising a realistic pathway for on-chip linear optical quantum simulation, quantum computation and quantum networks.

PACS numbers: 85.35.Be, 42.50.Ar, 42.82.-m, 42.50.Dv
Keywords: single photon source, integrated photonics, quantum dot, waveguides, resonance fluorescence, two-photon interference

Large scale implementations of quantum information processing (QIP) schemes are one of the major challenges of modern quantum physics. Building a platform successfully combing many qubits is a very demanding task, however it would provide a system capable to perform quantum simulations, quantum computing and secure quantum communication. In this regard, using single photons as qubits is a particularly appealing concept. Due to the photons low decoherence and the inherent possibility of low-loss transmission, they can be used for both quantum computing and quantum communication applications [1]. Over the last decade, there have been extensive experimental efforts towards realizing large-scale optical QIP systems. A vast majority of these implementations, such as linear optics quantum computing [2], boson sampling [3] or quantum repeater schemes [4] involve a two-photon interference effect, where a complete wavepacket overlap of single photons at the beam splitter is required. This feature demands photons, which are indistinguishable in terms of energy, bandwidth, polarization and arrival time at the beam splitter. Consequently, sources of indistinguishable single photons are one of the central resources for a large scale experimental realization of the optical QIP devices.

Among different kinds of emitters quantum dots (QDs) coupled to photonic structures have been shown to be one of the brightest single photon sources (SPS) [5–7], which under resonant excitation conditions [7–9] can reach simultaneously indistinguishabilities higher than 95%, single photon purities better than 99% and extraction efficiencies as high as 65-79% [7, 10–13]. Further, by applying advanced semiconductor micro-processing technologies it is possible to fabricate devices where QD electronic properties can be dynamically shaped by strain [14, 15] or electric [16, 17] fields. The optical quality of such sources allowed already for demonstration of on-demand CNOT-gates [18–20], heralded entanglement between distant hole spins [21] or the recent realization of 3-,4- and 5-photon boson sampling [22, 23].

It is believed that future steps towards large scale quantum optics should ensure the full on-chip scalability of SPSs [6, 24]. A natural system towards this goal are integrated circuits, where QD SPSs can be homogeneously [25–29] or heterogeneously [30–32] integrated on a single chip. In this approach light can be directly coupled into in-plane waveguides (WGs) and combined with other functionalities on a chip such as phase shifters [33, 34], beam splitters [25, 32, 35], filters [31, 36], detectors [29, 37] and other devices for light propagation, manipulation and detection on a single photon level.

By utilizing this idea near-unity coupling efficiency of a QD emitter to waveguide device was already achieved [26, 28, 38, 39], showing the undeniable potential of this concept. In addition, integrated circuits allow to spatially separate excitation and detection spots, which straightforwardly enables applying resonant driving schemes to slow-down decoherence processes and reduce on-demand emission time-jitter. This technique was already applied to waveguide integrated QDs under both continuous-wave [40, 41] (CW) and pulsed [16, 42, 43] excitation. In particular, two-photon interference of subsequently emitted resonance fluorescence photons have been demonstrated recently [16, 43], however recorded indistinguishability values failed to reach requirements imposed by quantum optics applications [44].

One of the major issues in QD-based on-chip SPSs

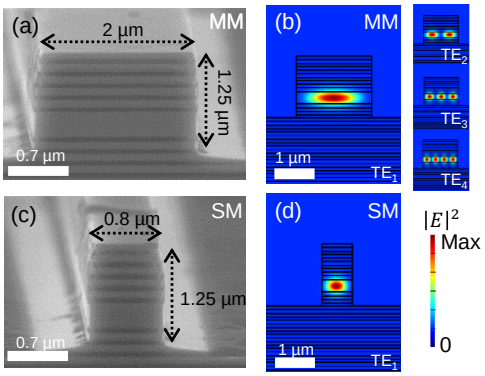


FIG. 1. Ridge waveguide image and mode profile. Scanning electron microscope images of the processed (a) multi-mode (MM) and (c) single-mode (SM) ridge waveguide structure. Optical power distribution profile for the TE (b) fundamental - $TE_1$ and higher order - $TE_{2-4}$ modes of MM and (d) fundamental $TE_1$ mode of SM waveguide at 930 nm wavelength.

is the loss of photon indistinguishability related to the charge fluctuation from nearby etched surfaces [40, 41]. This is true especially for small in size, complex structures such as photonic crystal [43] or nanobeam [16] waveguides. To diminish this effect a number of strategies can be employed. Firstly, the amount of surface states could be decreased by optimizing passivation of the etched surfaces [45]. Secondly, the charge environment could be stabilized by weak CW non-resonant optical illumination [46] or gating [11, 43]. Finally, the Purcell effect might be used to enhance the radiative emission rate and thus improve the photon indistinguishability in the presence of dephasing [10–12, 43, 47]. As we will show in this Letter, a simplified waveguide design with relatively large profile dimensions, keeping etched surfaces far away from QD, can be also very advantageous in this respect. By utilizing distributed Bragg reflectors (DBR) ridge waveguide design we fabricated SPSs which simultaneously meet the requirements of near perfect single photon purity and indistinguishability.

To evaluate the performance of our devices we performed resonance fluorescence experiments on In(Ga)As/GaAs QDs coupled to single-mode (SM) and multi-mode (MM) in-plane waveguides. The light confinement and guiding was achieved by DBRs in vertical and ridges defined in horizontal direction. Usage of DBRs WG instead of the GaAs WG slab approach allowed us to soften the waveguide profile dimensions allowing to achieve single-mode operation, while keeping a relatively high QD-waveguide light coupling efficiency (14-19% into one WG arm). To simulate the integrated circuit device operation, the QDs were excited resonantly from top of the waveguides, and the emitted photons were collected from the side facets after up to 1 mm travel distance on a chip. Under such conditions a significant reduction of the scattered laser intensity was achieved, enabling our MM (SM) waveguide device generation of record high on-chip 97.5% (95.0%) indistinguishable triggered single photons with a 99.1% (96.0%) single-photon purity and over 99% (98%) linear polarization. We believe, that this integrated SPSs can be readily scaled up demonstrating a realistic pathway for on-chip optical quantum processing.

To realize our waveguide integrated SPS we have grown In(Ga)As/GaAs QDs embedded in a low quality factor cavity (Q $\sim$ 200) based on DBRs. By performing three-dimensional finite-difference time-domain (FDTD) calculations we investigated different waveguide designs for maximized coupling efficiency. We found that 1.25-1.65 $\mu$m WG height and 0.6-2.0 $\mu$m width lay within optimal values and allow to achieve around 10-22% coupling efficiency into each WG arm (total 20-44%). Moreover, our DBR waveguides can be operated in the single-mode regime for WG widths as small as 0.9 $\mu$m at 900 nm cut-off wavelengths. Based on those considerations, we realized two types of ridge waveguides: (i) MM WGs with 2.0 x 1.25 $\mu m^2$ profile and (ii) SM WGs with 0.8 x 1.25 $\mu m^2$, for which we expect $\sim$14% and $\sim$19% QD coupling efficiency into one WG arm, respectively. We point out, that in principle the QD-emission coupling efficiency could be further improved by integration of DBR WGs with low-refractive index layers, while maintaining the mentioned relatively large size of WG profile. More details can be found in Supplemental Materials. Scanning electron microscope images of our fabricated MM and SM ridge waveguides are shown in Figures 1(a) and (c), respectively. Figures 1(b) and (d) show simulated optical mode profiles of the light field confined in our devices, calculated for the transverse-electric (TE) modes at 930 nm. In both cases the mode profiles are confined within the defined ridges, allowing for the single photon guiding along the chip. The modes are mainly concentrated in the GaAs cores and partially penetrate the top and bottom DBR mirrors.

Initially, both devices were characterized optically under non-resonant excitation conditions. Figure 2(a) and (c) show side collected photoluminescence (PL) spectra from a $QD_1$ and $QD_2$, respectively, under above-band gap CW pump (660 nm diode laser) from the top of the waveguide. In case of $QD_1$ coupled to a MM WG four intense emission lines are visible, where the one of interest centered at 1.3169 eV (marked with an arrow) was identified as a neutral exciton (X). The inset in Fig. 2(a) shows central peak intensity changes vs excitation power indicating a clear linear dependence. The remaining emission lines have been identified based on power- and top-detected-polarization-resolved PL as positively charged exciton ($X^+$), negatively charged exciton ($X^-$) and biexciton (XX) recombination from the same QD. Spectra for $QD_2$ coupled to the SM WG consists a single emission line centered at 1.3206 eV, identified as a charged exciton (CX). Both studied emission lines show a high

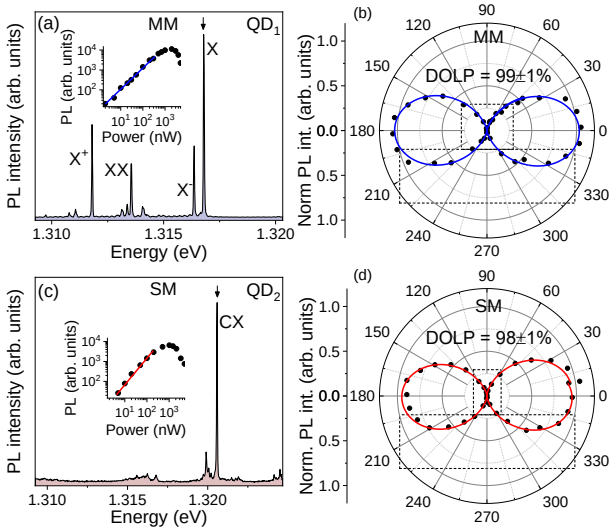


FIG. 2. Non-resonant photoluminescence. Side collected QD emission spectra recorded from (a) MM and (c) SM ridge WG device at 1 $\mu$W power CW excitation. Insets: intensity vs power dependencies of the marked with arrows PL peaks in log-log scale. Red/blue solid curve: fit with a power function showing linear dependence. Polarization characteristics of the (b) MM and (d) SM WG coupled QD PL emission, revealing 99±1% and 98±1% degree of linear polarization, respectively, oriented along the TE mode of the ridge waveguides.

degree of linear polarization (DOLP) of around 99±1% and 98±1% for $QD_1$ and $QD_2$, respectively, oriented in sample plane as shown in Figures 2(b) and (d). A high DOLP and its direction are related to the QDs dipole moments, which are mainly in-plane oriented and thus emitted photons mostly couple to and propagate in the TE waveguide mode.

Next, the devices characteristics were probed under pulsed s-shell resonant excitation. Figures 3(a) and (d) show side detected pulsed resonance fluorescence spectra displayed on a spectrometer at a temperature of 4.5 K. Since in our experimental configuration the excitation and collection spots are spatially separated by hundreds of micrometers, it allows us to rather readily suppress the stray laser photons scattered from the excitation area. This is usually not the case for short length waveguides as the laser light scattered from the excitation area might be collected within the numerical aperture of the detection objective. Additionally, the presence of low Q factor cavity in plane of the sample allowed us to more effectively excite the emitters and thus reduce powers needed for resonant driving. To further suppress the influence of laser light scattering on the single photon performance, the beam spot size as well as polarization was carefully controlled. By utilizing both the intrinsic (spatial separation) and polarization filtering we were able to obtain a signal-to-background (S/B) ratio of over 100 for MM and 30 for SM waveguide devices under $\pi$-pulse excitation. In fact, we believe that polarization filtering can be omitted for fully on-chip device operation.

In Figures 3(b) and (e) the resonance fluorescence intensity versus square root of the incident power are shown. Clear Rabi oscillations with visible damping for both QDs are observed, which is due to coherent control of the particular QD's two-level systems coupled to phonon bath [48]. The emission intensities in both cases reaches the maximum for $\pi$-pulse with laser powers of 440 nW and 160 $\mu$W for $QD_1$ and $QD_2$, respectively. The significantly larger pump power required to reach $\pi$-pulse for $QD_2$ is most likely related to the smaller size of the waveguide in respect to the laser beam spot size, as well as a slight energy detuning from the planar cavity resonance. The resonance fluorescence intensity of around 10 kcps (3.5 kcps) was observed on the avalanche photo-diode detector (setup efficiency ~2%) at $\pi$-pulse for a MM (SM) device, which corresponds to ~0.6% (~0.2%) total photon extraction efficiency from a QD collected by the first lens, and ~12% (~2%) coupling efficiency into one WG arm (lower bound estimated based on 95% and 90% losses due to the out-coupling). It needs to be noted that the design of the WGs for the high out-coupling into external collection optics was not optimized, since ultimately all single photon processing is supposed to be performed on-chip. Under $\pi$-pulse excitation the time-resolved resonance fluorescence measurements have been performed. The recorded fluorescence decay time traces shown in Fig. 3(c) and (f) demonstrate

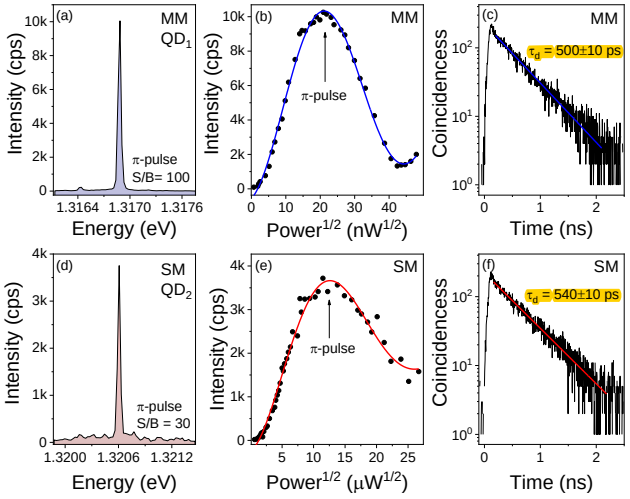


FIG. 3. Pulsed resonance fluorescence. Side collected QD emission spectra from (a) MM and (d) SM waveguide device under $\pi$-pulse excitation. (b),(e) Signal intensity versus square root of incident power. Solid red/blue curve: fit with a dumped sinusoidal function. (c),(f) Time-resolved resonance fluorescence measurement under $\pi$-pulse pumping. Red/blue solid curves: fit using a mono-exponential decay function with time constants of 500±10 ps and 540±10 ps for MM and SM device, respectively.

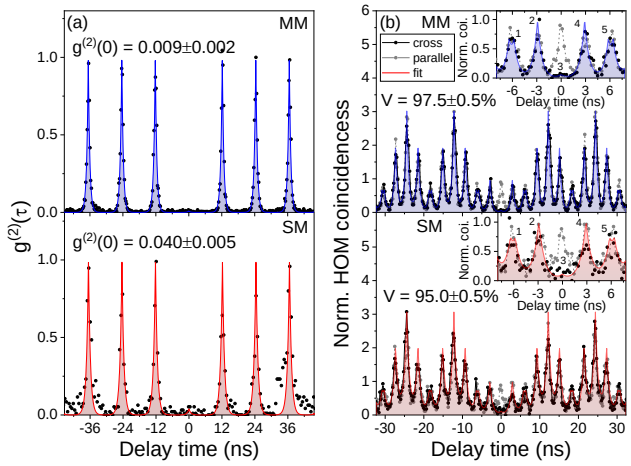


FIG. 4. Single photon generation and two photon interference under resonant $\pi$-pulse excitation. (a) Side collected resonance fluorescence intensity-correlation histogram recorded for $QD_1$ coupled to MM WG (upper panel) and $QD_2$ coupled to SM WG (lower panel). $g^{(2)}(0)$ values are calculated from the integrated photon counts, while the uncertainty is based on the standard deviation of the Poissonian peak counts. (b) Two-photon interference HOM histogram recorded for the 3 ns time separated co- (black points) and cross-polarized (grey points) single photons recorded for $QD_1$ (upper panel) and $QD_2$ (lower panel). Red/blue solid curves: fits based on two-sided exponential decay functions.

clear mono-exponential decays with the time constants of 500±10 ps and 540±10 ps for $QD_1$ and $QD_2$, respectively.

In order to characterize purity and indistinguishability of our SPSs auto-correlation and two-photon interference experiments have been performed on the resonance fluorescence signal filtered out from a broader laser profile and phonon sidebands. In Fig. 4(a) second order correlation function histograms recorded in Hanbury Brown and Twiss (HBT) configuration under $\pi$-pulse excitation for $QD_1$ and $QD_2$ are shown. In both cases, nearly vanishing multi-photon emission probabilities at zero delays have been recorded with $g^{(2)}(0) = 0.009 \pm 0.002$ and $g^{(2)}(0) = 0.04 \pm 0.005$ for $QD_1$ and $QD_2$, respectively. The shape of all the peaks exhibits a clear two-sided mono-exponential decay with a time constant corresponding to the decay time recorded directly in the time-resolved resonance fluorescence measurements.

To study the indistinguishability of the emitted photons the QDs were excited twice every repetition cycle (12.2 ns) by a pair of pulses separated by 3 ns. Two subsequently emitted photons are then introduced into a 3 ns unbalanced interferometer where a delay between them is compensated in order to superimpose single photon pulses on the beam splitter [5]. If the two photons are perfectly indistinguishable they will always exit the same but a random output port, which is quantitatively translated into the two-coincidences correlation dip at a zero delay. Hong-Ou-Mandel (HOM) correlation histograms obtained for the two considered photon sources are presented in Figure 4(b) in upper ($QD_1$) and lower ($QD_2$) panels. The histograms consist of a set of five 3 ns delayed peak clusters separated by the repetition time of the laser (first and last peak of the neighboring clusters are superimposed). The central cluster [insets in Figure 4(b)] describes coincidence events related to the single-photons traveling through different paths of the interferometer. This is described in detail in the Supplemental Materials. In order to evaluate the zero delay peak (no. 3) area in respect to the neighboring peaks (no. 2 and 4) the experimental data have been fitted with the two-side exponential decay functions. Upon this procedure the two-photon HOM interference visibility of 0.975±0.005 for $QD_1$ and 0.950±0.005 for $QD_2$ have been obtained after correcting for HOM setup imperfections such as beam-splitting ratio (R/T = 1.15) and contrast of the Mach-Zehnder-interferometer (1-$\varepsilon$ = 0.99)[5, 13].

It was recently demonstrated, that single photon emission purity and indistinguishability in resonantly excited two-level systems is intrinsically limited by the re-excitation process[13, 49]. Specifically, it was shown that the laser excitation pulse-length $\tau_{pulse}$ sets the lower bounds of the HBT and HOM experimental two photon coincidences probability, and thus $g^{(2)}(0)$ and visibility values obtainable for a given SPS with characteristic emission time $\tau_{emitter}$. Based on reference [13] those bounds can be calculated following the linear dependence $0.4 \cdot \tau_{pulse}/\tau_{emitter}$, which in our case limits $g^{(2)}(0)$ (visibility) to 0.0016 (0.9984) and 0.0015 (0.9985) for $QD_1$ and $QD_2$, respectively. Since the experimentally obtained single-photon purity values are significantly above the aforementioned limits, we believe their dominant component might be non-filtered residual scatter of the laser pulse from sample surface, which we does not take into account in HBT and HOM data analysis.

Imperfect efficiency and indistinguishability of SPSs is related to the problem of optical quantum computation under a degree of experimental error. There have been a number of promising proposals of linear optical quantum computing that are robust against imperfect SPSs and inefficient detectors. In particular, it was shown, that fault-tolerant quantum computation can be performed if the two-photon gate operation error probability is lower than a 1% threshold value [50, 51]. In this regard we can calculate how the indistinguishability of input photons affects the two-photon gate performance assuming perfect beam-overlap, alignment, beam-splitters and no dark counts in single photon counting detection. In case of our MM (SM) waveguide QD source with 97.5% (95.0%) photons visibility a gate fidelity of 99.5% (99.1%) [52] is theoretically obtainable. Those values already surpass mentioned 1% precision threshold value, and in this context our work provides SPSs with photons visibility needed for scalable quantum technologies.

Another source of error in quantum optics, which is

far more dominant than gate fidelity is photon loss. This problem is associated with overall source and detectors efficiency, which product have to be greater than 2/3 in order to perform efficient fault-tolerant linear optical quantum computation [53]. In principle this efficiency threshold is very difficult to fulfill in any system, since every optical setup exhibit losses. In all on-chip platforms however, where single photons are generated, routed, manipulated and eventually detected within the same low loss photonic circuit, this efficiency threshold is likely to be fulfilled within near future.

In this context, essential next steps to make QD-based on-chip platform feasible for fully scalable quantum technologies would consist of (i) improving QD-waveguide circuit coupling efficiency while maintaining high degree of photons indistinguishability, (ii) introducing high-visibility and low-loss on-chip interferometers and phase shifters based on single-mode waveguides, and (iii) integrating with high efficiency superconducting detectors [6, 7, 24]. Such a system may at some point overcome the intrinsic limitations of the vertical devices, opening the possibility to create a scalable quantum integrated circuits operating at the single photon level.

In this Letter we have shown that our MM (SM) waveguide integrated SPS can generate photons with near-unity indistinguishability of 0.975±0.005 (0.950±0.005) along with the $g^{(2)}(0)$ value equal to 0.009±0.002 (0.040±0.005). We demonstrated single photon propagation of over hundreds of micrometers in waveguides and QD-WG coupling efficiency of ∼12% (∼2%) into one WG arm. In contrast to any other QD-based waveguide integrated SPS which has been demonstrated thus far [16, 43], our devices fulfill ultimate single photon purity and indistinguishability demands, imposed by boson sampling and linear optical quantum computing applications [44]. Performance of this source already outperforms any other on-chip integrated emitters including state-of-the-art heralded single photon spontaneous parametric down-conversion sources, where a maximum of 91% photons indistinguishability have been achieved at 4-5% source efficiency [54, 55]. We believe that our device could be straightforwardly integrated with advanced on-chip functionalities including reconfigurable and reprogrammable optical circuits [56] suitable for handling large scale multi-photon experiments. A potential of manufacturing such advanced quantum circuits combined with high purity indistinguishable SPS open a route towards fully integrated and thus scalable quantum information processing.

The authors thank Silke Kuhn for fabricating the structures, and Dominick Köck for calculating the electric field distribution in waveguides. Ł.D. acknowledges the financial support from Alexander von Humboldt Foundation. S.-H.K. acknowledges the financial support from National Research Foundation of Korea through the Korean Government Grant NRF-2016R1C1B2007007. We are furthermore grateful for the support by the State of Bavaria.

* lukasz.dusanowski@physik.uni-wuerzburg.de

[1] P. Kok and B. Lovett, *Introduction to Optical Quantum Information Processing* (Cambridge University Press, 2010).
[2] E. Knill, R. Laflamme, and G. J. Milburn, Nature **409**, 46 (2001).
[3] J. B. Spring, B. J. Metcalf, P. C. Humphreys, W. S. Kolthammer, X.-M. Jin, M. Barbieri, A. Datta, N. Thomas-Peter, N. K. Langford, D. Kundys, J. C. Gates, B. J. Smith, P. G. R. Smith, and I. A. Walmsley, Science **339**, 798 (2013).
[4] H.-J. Briegel, W. Dür, J. I. Cirac, and P. Zoller, Physical Review Letters **81**, 5932 (1998).
[5] C. Santori, D. Fattal, J. Vucković, G. S. Solomon, and Y. Yamamoto, Nature **419**, 594 (2002).
[6] I. Aharonovich, D. Englund, and M. Toth, Nature Photonics **10**, 631 (2016).
[7] P. Senellart, G. Solomon, and A. White, Nature Nanotechnology **12**, 1026 (2017).
[8] E. B. Flagg, A. Muller, J. W. Robertson, S. Founta, D. G. Deppe, M. Xiao, W. Ma, G. J. Salamo, and C. K. Shih, Nature Physics **5**, 203 (2009).
[9] S. Ates, S. M. Ulrich, S. Reitzenstein, A. Löffler, A. Forchel, and P. Michler, Physical Review Letters **103**, 167402 (2009).
[10] X. Ding, Y. He, Z. C. Duan, N. Gregersen, M. C. Chen, S. Unsleber, S. Maier, C. Schneider, M. Kamp, S. Höfling, C.-Y. Lu, and J.-W. Pan, Physical Review Letters **116**, 020401 (2016).
[11] N. Somaschi, V. Giesz, L. De Santis, J. C. Loredo, M. P. Almeida, G. Hornecker, S. L. Portalupi, T. Grange, C. Antón, J. Demory, C. Gómez, I. Sagnes, N. D. Lanzillotti-Kimura, A. Lemaítre, A. Auffeves, A. G. White, L. Lanco, and P. Senellart, Nature Photonics **10**, 340 (2016).
[12] S. Unsleber, Y.-M. He, S. Maier, S. Gerhardt, C.-Y. Lu, J.-W. Pan, M. Kamp, C. Schneider, and S. Höfling, Optics express **24**, 8539 (2016).
[13] K. A. Fischer, K. Müller, K. G. Lagoudakis, and J. Vučković, New Journal of Physics **18**, 113053 (2016).
[14] Y. Zhang, Y. Chen, M. Mietschke, L. Zhang, F. Yuan, S. Abel, R. Hühne, K. Nielsch, J. Fompeyrine, F. Ding, and O. G. Schmidt, Nano Letters **16**, 5785 (2016).
[15] R. Trotta, J. Martín-Sánchez, J. S. Wildmann, G. Piredda, M. Reindl, C. Schimpf, E. Zallo, S. Stroj, J. Edlinger, and A. Rastelli, Nature Communications **7**, 10375 (2016).
[16] G. Kiršanskė, H. Thyrrestrup, R. S. Daveau, C. L. Dreeßen, T. Pregnolato, L. Midolo, P. Tighineanu, A. Javadi, S. Stobbe, R. Schott, A. Ludwig, A. D. Wieck, S. I. Park, J. D. Song, A. V. Kuhlmann, I. Söllner, M. C. Löbl, R. J. Warburton, and P. Lodahl, Physical Review B **96**, 165306 (2017).
[17] T. B. Hoang, J. Beetz, M. Lermer, L. Midolo, M. Kamp, S. Höfling, and A. Fiore, Optics Express **20**, 21758 (2012).
[18] M. A. Pooley, D. J. P. Ellis, R. B. Patel, A. J. Bennett,

K. H. A. Chan, I. Farrer, D. A. Ritchie, and A. J. Shields, Applied Physics Letters **100**, 211103 (2012).
[19] O. Gazzano, M. P. Almeida, A. K. Nowak, S. L. Portalupi, A. Lemaître, I. Sagnes, A. G. White, and P. Senellart, Physical Review Letters **110**, 250501 (2013).
[20] Y.-M. He, Y. He, Y.-J. Wei, D. Wu, M. Atatüre, C. Schneider, S. Höfling, M. Kamp, C.-Y. Lu, and J.-W. Pan, Nature Nanotechnology **8**, 213 (2013).
[21] A. Delteil, Z. Sun, W.-b. Gao, E. Togan, S. Faelt, and A. Imamoglu, Nature Physics **12**, 218 (2015).
[22] H. Wang, Y.-M. He, Y.-H. Li, Z.-E. Su, B. Li, H.-L. Huang, X. Ding, M.-C. Chen, C. Liu, J. Qin, J.-P. Li, Y.-M. He, C. Schneider, M. Kamp, C.-Z. Peng, S. Höfling, C.-Y. Lu, and J.-W. Pan, Nature Photonics **11**, 361 (2017).
[23] J. C. Loredo, M. A. Broome, P. Hilaire, O. Gazzano, I. Sagnes, A. Lemaitre, M. P. Almeida, P. Senellart, and A. G. White, Physical Review Letters **118**, 130503 (2017).
[24] C. P. Dietrich, A. Fiore, M. G. Thompson, M. Kamp, and S. Höfling, Laser & Photonics Reviews **10**, 870 (2016).
[25] K. D. Jöns, U. Rengstl, M. Oster, F. Hargart, M. Heldmaier, S. Bounouar, S. M. Ulrich, M. Jetter, and P. Michler, Journal of Physics D: Applied Physics **48**, 085101 (2015).
[26] A. Enderlin, Y. Ota, R. Ohta, N. Kumagai, S. Ishida, S. Iwamoto, and Y. Arakawa, Physical Review B **86**, 075314 (2012).
[27] A. Schwagmann, S. Kalliakos, I. Farrer, J. P. Griffiths, G. A. C. Jones, D. A. Ritchie, and A. J. Shields, Applied Physics Letters **99**, 261108 (2011).
[28] M. Arcari, I. Söllner, A. Javadi, S. Lindskov Hansen, S. Mahmoodian, J. Liu, H. Thyrrestrup, E. H. Lee, J. D. Song, S. Stobbe, and P. Lodahl, Physical Review Letters **113**, 093603 (2014).
[29] G. Reithmaier, M. Kaniber, F. Flassig, S. Lichtmannecker, K. Müller, A. Andrejew, J. Vučković, R. Gross, and J. J. Finley, Nano Letters **15**, 5208 (2015).
[30] M. Davanco, J. Liu, L. Sapienza, C.-Z. Zhang, J. V. De Miranda Cardoso, V. Verma, R. Mirin, S. W. Nam, L. Liu, and K. Srinivasan, Nature Communications **8**, 889 (2017).
[31] A. W. Elshaari, I. E. Zadeh, A. Fognini, M. E. Reimer, D. Dalacu, P. J. Poole, V. Zwiller, and K. D. Jöns, Nature Communications **8**, 379 (2017).
[32] J.-H. Kim, S. Aghaeimeibodi, C. J. K. Richardson, R. P. Leavitt, D. Englund, and E. Waks, Nano Letters **17**, 7394 (2017).
[33] L. Midolo, S. L. Hansen, W. Zhang, C. Papon, R. Schott, A. Ludwig, A. D. Wieck, P. Lodahl, and S. Stobbe, Opt. Express **25**, 33514 (2017).
[34] J. Wang, A. Santamato, P. Jiang, D. Bonneau, E. Engin, J. W. Silverstone, M. Lermer, J. Beetz, M. Kamp, S. Höfling, M. G. Tanner, C. M. Natarajan, R. H. Hadfield, S. N. Dorenbos, V. Zwiller, J. L. O'Brien, and M. G. Thompson, Optics Communications **327**, 49 (2014).
[35] N. Prtljaga, R. J. Coles, J. O'Hara, B. Royall, E. Clarke, A. M. Fox, and M. S. Skolnick, Applied Physics Letters **104**, 231107 (2014).
[36] N. C. Harris, D. Grassani, A. Simbula, M. Pant, M. Galli, T. Baehr-Jones, M. Hochberg, D. Englund, D. Bajoni, and C. Galland, Physical Review X **4**, 041047 (2014).
[37] M. Kaniber, F. Flassig, G. Reithmaier, R. Gross, and J. J. Finley, Applied Physics B **122**, 115 (2016).
[38] T. Lund-Hansen, S. Stobbe, B. Julsgaard, H. Thyrrestrup, T. Sünner, M. Kamp, A. Forchel, and P. Lodahl, Physical Review Letters **101**, 113903 (2008).
[39] P. Stepanov, A. Delga, X. Zang, J. Bleuse, E. Dupuy, E. Peinke, P. Lalanne, J.-M. Gérard, and J. Claudon, Applied Physics Letters **106**, 041112 (2015).
[40] M. N. Makhonin, J. E. Dixon, R. J. Coles, B. Royall, I. J. Luxmoore, E. Clarke, M. Hugues, M. S. Skolnick, and A. M. Fox, Nano Letters **14**, 6997 (2014).
[41] S. Kalliakos, Y. Brody, A. J. Bennett, D. J. P. Ellis, J. Skiba-Szymanska, I. Farrer, J. P. Griffiths, D. A. Ritchie, and A. J. Shields, Applied Physics Letters **109**, 151112 (2016).
[42] M. Schwartz, U. Rengstl, T. Herzog, M. Paul, J. Kettler, S. L. Portalupi, M. Jetter, and P. Michler, Optics Express **24**, 3089 (2016).
[43] F. Liu, A. J. Brash, J. O'Hara, L. M. P. P. Martins, C. L. Phillips, R. J. Coles, B. Royall, E. Clarke, C. Bentham, N. Prtljaga, I. E. Itskevich, L. R. Wilson, M. S. Skolnick, and A. M. Fox, Nature Nanotechnology **13**, 835 (2018).
[44] J.-W. Pan, Z.-B. Chen, C.-Y. Lu, H. Weinfurter, A. Zeilinger, and M. Żukowski, Reviews of Modern Physics **84**, 777 (2012).
[45] D. Press, K. De Greve, P. L. McMahon, T. D. Ladd, B. Friess, C. Schneider, M. Kamp, S. Höfling, A. Forchel, and Y. Yamamoto, Nature Photonics **4**, 367 (2010).
[46] A. Majumdar, E. D. Kim, and J. Vučković, Physical Review B **84**, 195304 (2011).
[47] J. Iles-Smith, D. P. S. McCutcheon, A. Nazir, and J. Mørk, Nature Photonics **11**, 521 (2017), 1612.04173.
[48] J. Förstner, C. Weber, J. Danckwerts, and A. Knorr, Physical Review Letters **91**, 127401 (2003).
[49] L. Hanschke, K. A. Fischer, S. Appel, D. Lukin, J. Wierzbowski, S. Sun, R. Trivedi, J. Vučković, J. J. Finley, and K. Müller, npj Quantum Information **4**, 43 (2018), 1801.01672.
[50] A. G. Fowler, A. M. Stephens, and P. Groszkowski, Physical Review A **80**, 052312 (2009).
[51] E. Knill, Nature **434**, 39 (2005), 0410199 [quant-ph].
[52] Y.-J. Wei, Y.-M. He, M.-C. Chen, Y.-N. Hu, Y. He, D. Wu, C. Schneider, M. Kamp, S. Höfling, C.-Y. Lu, and J.-W. Pan, Nano Letters **14**, 6515 (2014).
[53] M. Varnava, D. E. Browne, and T. Rudolph, Physical Review Letters **100**, 060502 (2008).
[54] X.-L. Wang, L.-K. Chen, W. Li, H.-L. Huang, C. Liu, C. Chen, Y.-H. Luo, Z.-E. Su, D. Wu, Z.-D. Li, H. Lu, Y. Hu, X. Jiang, C.-Z. Peng, L. Li, N.-L. Liu, Y.-A. Chen, C.-Y. Lu, and J.-W. Pan, Physical Review Letters **117**, 210502 (2016).
[55] F. Kaneda and P. G. Kwiat, arXiv , 1803.04803 (2018), arXiv:1803.04803v1.
[56] J. Carolan, C. Harrold, C. Sparrow, E. Martín-López, N. J. Russell, J. W. Silverstone, P. J. Shadbolt, N. Matsuda, M. Oguma, M. Itoh, G. D. Marshall, M. G. Thompson, J. C. F. Matthews, T. Hashimoto, J. L. O'Brien, and A. Laing, Science **349**, 711 (2015).